Student Paper

Comparative study of E- and D-mode InAlN/AlN/GaN HEMTs with f_T near 200 GHz

Berardi Sensale-Rodriguez[a*], Jia Guo[a], Ronghua Wang[a], Guowang Li[a], Tian Fang[a], Paul Saunier[b], Andrew Ketterson[b], Michael Schuette[b], Xiang Gao[c], Shiping Guo[c], Yu Cao[d], Oleg Laboutin[d], Wayne Johnson[d], Gregory Snider[a], Patrick Fay[a], Debdeep Jena[a], and Huili (Grace) Xing[a**]

[a]*Department of Electrical Engineering, University of Notre Dame, USA,* [*]*bsensale@nd.edu*
[**]*hxing@nd.edu,* [b] *Triquint Semiconductor, USA,* [c] *IQE RF LLC, USA,* [d]*Kopin Corporation, USA.*

We report on the 172/180 GHz (f_T/f_{max}) E-mode InAlN/AlN/GaN HEMTs with a recess-etched gate footprint of 33 nm. To develop further scaling strategies [1], comparative studies were carried out on E- and D-mode HEMTs with f_T near 200 GHz at both room (RT) and cryogenic temperatures (LT). Delay component analysis indicates that the speed of the E-mode device is dominated by parasitic delays, and that the electron velocity in the E-mode is about 2/3 of that in D-mode, most likely steming from mobility degradation during gate recess etch.

Schematic cross-sections of the studied devices are shown in Fig.1. The structure of the E-mode devices, for which a recess-etched gate foot length of 33 nm and a 120-nm SiO_2 passivation were adopted, is presented in Fig.1(a). InAlN and InAlGaN D-mode devices were studied to investigate the effect of carrier mobility (Fig.1.(b)-(c)). Gate lengths from 250 nm to 50 nm were fabricated with 5-6 nm ALD Al_2O_3 passivation for the D-mode HEMTs.

TLM measurements showed a contact resistance R_c of 0.36, 0.36, 0.35 ohm-mm and a sheet resistance R_{sh} of 276, 190, 292 ohm/sq. at RT for the fully fabricated E-mode, D-mode quaternary and ternary barrier devices, respectively. The lower sheet resistance of the quaternary HEMT is due to the higher carrier mobility [2], 1790 cm^2/Vs (1.8x10^{13} cm^{-2}) in comparison to 983 cm^2/Vs (2.23x10^{13} cm^{-2}) in the ternary HEMT, determined by Hall effect measurements.

Common-source family of I-Vs and transfer characteristics were measured for all the devices at RT and LT. Both 77K and 4K were used but no significant differences in device performance were observed since the carrier mobility is mostly constant in this temperature range. All the devices showed a decrease in the on-resistance (~10-15%) and an increase in the extrinsic DC g_m (~15-20%) at LT, as shown in Fig. 2. TLM and coldFET measurements showed that the expected R_s+R_d decreased by 25-35% at LT (i.e., from 1.1 to 0.7 ohm-mm in the InAlN D-mode devices and from 0.8 to 0.6 ohm-mm in the E-mode devices). But the substantial increase in the extrinsic DC g_m from RT to LT didn't translated into a commensurate increase in f_T; as can be seen in Fig. 3, f_T increased about 20% for the 120-nm D-mode, and between 10 and 15% for all the other devices. Delay time analysis was performed in order to provide insight into this observation using both the traditional Moll analysis [3] as well as the method described by Suemitsu [4] (Fig. 4), where the parasitic delay associated with the parasitic access resistances can be subtracted. The delay distribution by applying Suemitsu's method shows that the improvement in f_T at LT for sub-100 nm gate devices is mainly due to a reduction in parasitic delay stemming from mobility enhancement and thus reduction in access resistances. Longer gates, e.g. 120-nm D-mode, exhibited a small decrease in gate transit delay (consistent with electron peak velocity being proportional to $\sqrt{\mu_0}$ [2]). Strong short channel effects may also be responsible for observing no improvement in the gate delay at LT for sub-100-nm devices. This study suggests that 300-GHz E-mode GaN HEMTs are achievable by adopting novel passivation schemes offering lower C_{gd} [5], regrown contacts with low R_c [6], self-aligned topologies to curb drain delay and back barriers to mitigate short channel effects.

References

[1] Y. Tang et al., "High-performance monolithically integrated E/D mode InAlN/AlN/GaN HEMTs for mixed-signal applications," in IEDM Tech. Dig., 2010, pp. 30.4.1–30.4.4.

[2] R. Wang, et al., "Enhancement-mode InAlN/AlN/GaN HEMTs with 10^{-12} A/mm leakage current and 10^{12} on/off current ratio," IEEE Electron Device Lett., vol. 32, no. 3, pp. 309–311, Mar. 2011.

[3] N. Moll, et al. "Pulse-doped AlGaAs/InGaAs pseudomorphic MODFETs," IEEE Trans.

Electron Devices, vol. 35, no. 7, pp. 879–896, Jul. 1988.

[4] T. Suemitsu, "An intrinsic delay extraction method for Schottky gate field effect transistors," IEEE Electron Device Lett., vol.25, no.10, pp. 669- 671, Oct. 2004.

[5] R. Wang et al., "210 GHz InAlN/GaN HEMTs with dielectric free passivation," IEEE Electron Device Lett., vol. 32, no. 7, pp. 892–894, Jul. 2011.

[6] J. Guo, et al., "Metal-face InAlN/AlN/GaN high electron mobility transistors with regrown ohmic contacts by molecular beam epitaxy," Phys. Status Solidi A, vol. 208, no. 7, pp. 1617-1619, Jul. 2011.

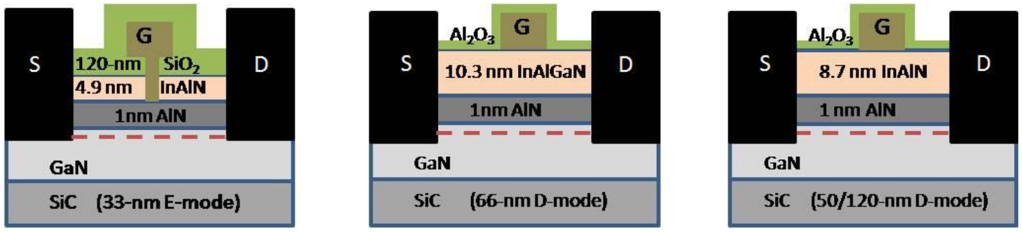

(a) **(b)** **(c)**

Fig. 1. Schematic of the devices analyzed in this study. The gate length and RT-f_T for the E-mode devices are 33 nm and 172 GHz; and for the quaternary InAlGaN barrier and ternary InAlN barrier HEMTs are 66-nm and 210 GHz, 50/120 nm and 197/176 GHz, respectively.

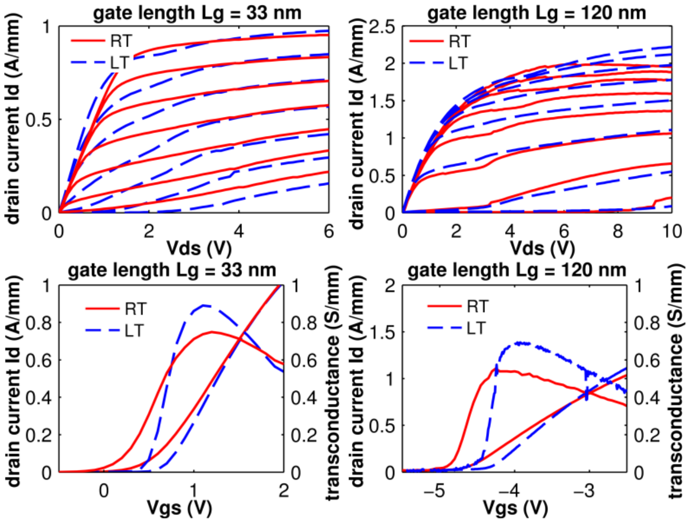

Fig. 2. Representative common-source family of I-Vs and transfer characteristics for the 33-nm E-mode, and 120-nm D-mode InAlN/AlN/GaN HEMTs.

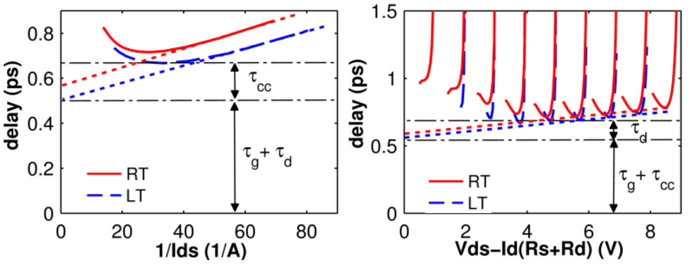

Fig. 4. Representative delay component analysis of the HEMTs using Suemitsu's method [4].

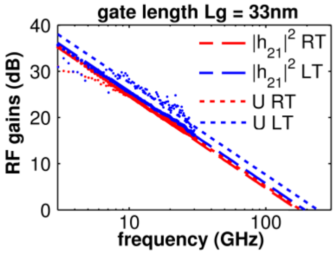

Fig. 3. RF gains as a function of frequency for the 33-nm HEMT. At LT f_T/f_{max} of the 33 -nm E-mode device increased from 172/180 GHz to 191/240 GHz.

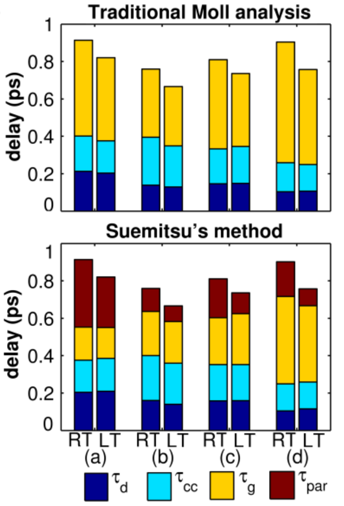

Fig. 5. Delay analysis of the 33-nm E-mode (a) and the 66-nm quaternary (b), 50-nm ternary (c) and 120-nm ternary (d) D-mode HEMTs.